

A Comparison of the Series-Parallel Compensation Type DC-DC Converters using both a Fuel Cell and a Battery

Koji Orikiawa

Student Member, IEEE

Nagaoka University of Technology
1603-1 Kamitomioka-machi, Nagaoka-city, Niigata, Japan
orikawa@stn.nagaokaut.ac.jp

Jun-ichi Itoh

Member, IEEE

Nagaoka University of Technology
1603-1 Kamitomioka-machi, Nagaoka-city, Niigata, Japan
itoh@vos.nagaokaut.ac.jp

Abstract -- This paper describes the comparison of two proposed circuits in terms of the efficiency. Series-parallel compensation type DC-DC converters have been proposed for hybrid power supplies using both fuel cell and battery. The output voltage is controlled by a series converter that regulates only the differential voltage between the fuel cell voltage and the output voltage. Although the load condition is changed, the variation of the fuel cell current is suppressed by a battery through operation of the parallel converter. The experimental results confirmed that the proposed circuit could achieve maximum efficiency point of 98.8% and 99.1% in the small differential voltage region, respectively. In addition, the loss distribution of the each proposed circuit is clarified by the loss analysis. As a result, it is confirmed that the optimizing of the reactor is required in order to improve the efficiency of the proposed circuit.

Index Terms—DC-DC power conversion, Fuel cells, Reactors

I. INTRODUCTION

Recently, fuel cell systems are being developed as a new power supply for mobile devices because the mobile electronic devices are developed with increasingly high performance and functionality, accompanied by larger power consumption and the demand for longer operation times. A resonant type converter, which use zero voltage switching or zero current switching, is one of the most effective circuit topologies to obtain high efficiency [1-2]. However, the conventional DC-DC converter converts all the power regardless of the output voltage because the conventional converter is connected in parallel to a power supply and a load.

Many DC-DC converter circuit topologies for fuel cell applications have been studied in order to obtain high efficiency [3-5]. However, a fuel cell requires a battery or an electric double layer capacitor (EDLC) to compensate the dynamic response, because fuel cell cannot respond to a quick load fluctuation. A hybrid power supply using both the fuel cell and battery also requires the following; high efficiency, downsizing, and quick response to load fluctuations. Nowadays, hybrid power supplies using both the batteries and fuel cells are being actively studied [6-8].

In order to achieve these requests, series-parallel

compensation type DC-DC converters have been proposed for hybrid power supplies using both fuel cell and battery [9]. The proposed system consists of a series converter and a parallel converter to control the input current and the output voltage respectively. In the proposed circuit, the series converter generates a positive and negative voltage to achieve boost and buck operation. On the other hand, the parallel converter with a battery compensates the quick response according to the load fluctuations. A control strategy is also proposed to achieve the quick response over the load and to slow down the power fluctuation of the fuel cell.

This paper discusses about the comparison of two proposed series-parallel type DC-DC converters in order to clarify the advantages of each converters. Two type of the series-parallel compensation type converters are proposed depending on the location of a reactor in the converter. First, the principle of the proposed DC-DC converter is introduced. In the proposed converter, the output power is directly provided by the fuel cell without any switching operation. Besides, the power rating of the DC-DC converter can be drastically reduced. As a result, high efficiency is obtained. Next, the configuration comparison of the proposed circuits in terms of the efficiency is described. After that, the loss analysis clarified the loss distribution of the each proposed circuit. As a result, it is confirmed that the optimizing of the reactor is needed in order to improve the efficiency of the proposed circuit. In addition, the design of the reactors is described with considering a suppression method on the ripple current of the fuel cell where the ripple will influence the lifetime of the fuel cell. Finally, the experimental results are presented to demonstrate the advantages of the proposed converter.

II. CONCEPT OF PROPOSED CIRCUIT

A. Series compensation

Fig. 1(a) presents a block diagram of a conventional buck-boost chopper. These converters convert all the input power, which is not dominated by the relations between the input and output voltage. For example, in a conventional buck-

boost chopper, which consists of a energy storage reactor and a single switching device, when the input voltage V_{in} is closed to the output voltage V_{outs} , the duty ratio D of a single stage buck boost chopper is obtained by (1), using the on time t_{on} , and off time t_{off} .

$$D = \frac{t_{on}}{t_{on} + t_{off}} = \frac{V_{out}}{V_{in} + V_{out}} = 0.5 \quad (1)$$

In this case, switching devices should be operated regardless of the relations between the input voltage and the output voltage. Besides, the energy for the output should be charge by an intermediate reactor or capacitor. As a result, the efficiency will be decreased.

Fig. 1(b) shows a block diagram of the series compensation converter, which is connected in series to the power supply. The series converter outputs only the differential voltage between the fuel cell voltage and the output voltage. Therefore, when the fuel cell voltage is closed to the output voltage, the output power is directly provided by the fuel cell without any switching operation; therefore, high efficiency is obtained by the series compensation circuit, although fluctuation of the output current directly becomes a fluctuation of the fuel cell current due to the series connection, which will decrease the lifetime of the fuel cell. A voltage ripple of the fuel cell occurs due to the internal impedance in the fuel cell.

B. Series-parallel compensation

Fig. 1(c) shows a block diagram of the proposed series-parallel compensation converter. In the proposed circuit, the parallel converter is connected in parallel to the fuel cell. When the output power is constant, the parallel converter does not operate, and the series compensation method can obtain high efficiency. The output voltage V_{out} is obtained by (2), using the series converter output voltage V_{conv} and the fuel cell voltage V_{fc} .

$$V_{out} = V_{fc} \pm V_{conv} \quad (2)$$

When the load condition has changed, the parallel converter will compensate the quick variation of the fuel cell current. The fluctuation of the output power is compensated by the battery through the operation of that parallel converter. In addition, when the battery voltage is decreased or overcharged, either the battery will be charged from the fuel cell or the battery supplies the power to the load through the operation of that parallel converter.

III. PROPOSED CIRCUIT

Fig. 2(a) shows the proposed circuit that a reactor L_{fc} is connected in series to the fuel cell in order to suppress the ripple current of the fuel cell. Further, the reactor is also used as a boost reactor when the boost mode is selected. In Fig. 2(a), the series converter is operated as a boost converter and a step-down converter. The output of the parallel converter is connected to the negative terminal of the fuel cell. The proposed circuit requires only two reactors, where the

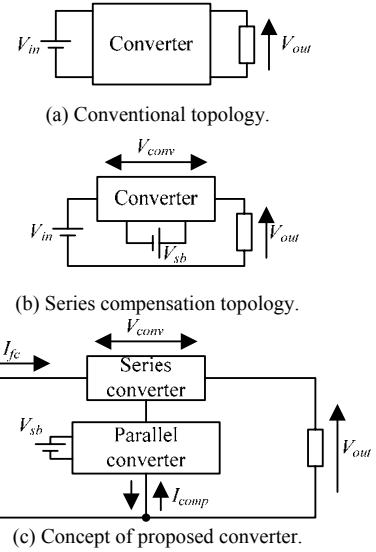


Fig. 1. Block diagrams of proposed converter in comparison with a conventional circuit.

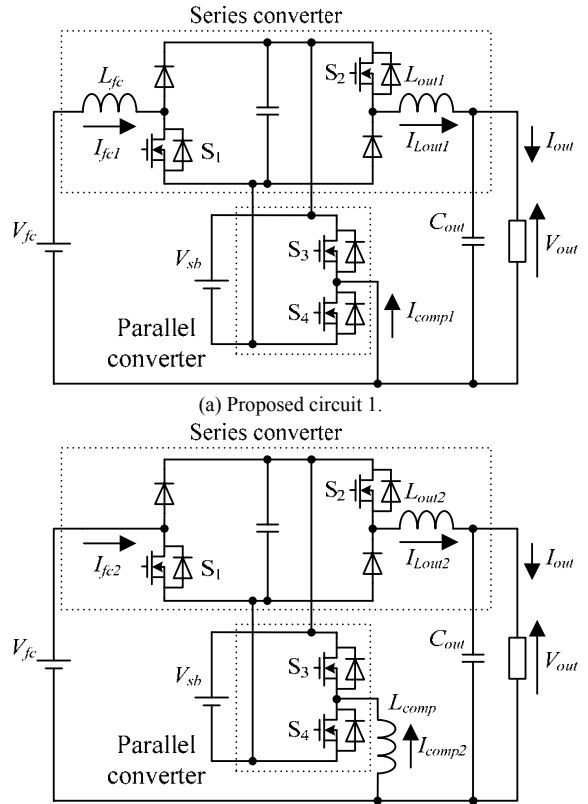


Fig. 2. Proposed circuit.

conventional circuit needs to use three reactors.

Fig. 2(b) shows another type of the proposed circuit that a reactor L_{comp} is connected to the parallel converter, in order to reduce the conduction loss of the reactor in comparison to Fig. 2(a). In Fig. 2(a), reactor current I_{fc} of L_{fc} is the sum of

the output current I_{Lout} and compensation current I_{comp} . Therefore, the conduction loss of the reactor will be increased. On the other hand, in Fig. 2(b), the reactor current of L_{comp} is lower than the output current due to only fluctuation components of the output power. Therefore, the conduction loss of the reactor L_{comp} can be reduced. It is noted that, the battery voltage must be higher than the fuel cell voltage to prevent a rush current from the fuel cell to the battery in the proposed circuit 1 and 2.

IV. CONTROL STRATEGY

Fig. 3 shows the control diagrams of the proposed circuit. The proposed control method has two loops; the inner loop is for controlling the fuel cell current and the parallel converter current. As for the outer loop, it is for the output voltage control. The same control strategy can be applied to the proposed circuit 1 and 2 because the fundamental operation is the same.

Operation between the series and parallel converter is constrained by the load condition in order to reduce the converter loss. In boost mode, the series converter works as a boost converter. In this case, the battery supplies the power to the load, because the differential voltage is positive. In buck mode, the series converter operates as a buck converter. In this case, the battery is charged from the fuel cell, since the differential voltage is negative. The switches S_3 and S_4 are for the parallel converter. The parallel converter works only when the load is fluctuating. The parallel converter will be started when the load fluctuation is detected by the window comparator and is stopped after the time runs longer than the time constant of the LPF and HPF.

The current command is divided into the fuel cell current command and the compensation current command. Low pass filters (LPF) and high pass filters (HPF) are used to divide the current command. The LPF is used to separate the fundamental current fluctuation, for the slow response of the fuel cell. The HPF is used to separate the transient current fluctuation for the fast response of the battery. The HPF functions simultaneously with the LPF filter, as shown in Fig. 3. The time constants of the LPF and HPF are set to the same value.

The frequency responses of the LPF and HPF do not influence the output current response, as explained by the following. The relations between each current can be expressed by (3), using the fuel cell current I_{fc} and the parallel converter current I_{comp} .

$$I_{Lout} = I_{fc} + I_{comp} \quad (3)$$

The fuel cell current command I_{fc}^* and the parallel converter current command I_{comp}^* are obtained by (4) and (5)

$$I_{fc}^* = \frac{1}{1+sT} I_{Lout}^* \quad (4) \quad I_{comp}^* = \frac{sT}{1+sT} I_{Lout}^* \quad (5)$$

where T is the time constant of the filter and I_{Lout}^* is the output current command. Therefore, the output current is obtained by (6).

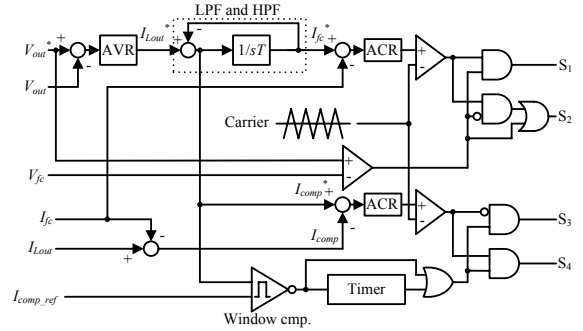


Fig. 3. Control diagrams for the proposed circuit.

$$I_{Lout} = G_1(s)I_{fc}^* + G_2(s)I_{comp}^* \quad (6)$$

where $G_1(s)$ and $G_2(s)$ are the transfer functions of the fuel cell current control and the parallel converter current control, respectively.

In addition, the output current is expressed by (7) when both the design values of the current regulator for the fuel cell and parallel converter are the same.

$$I_{Lout} = G(s)I_{Lout}^* \quad (7)$$

where $G(s)$ is the transfer function of the output current control. That is, the time constant of the LPF or HPF does not appear in the transfer function of the output current control. In addition, the operation of the parallel converter is started by variation of the parallel converter current command I_{comp}^* . Then, operation of the parallel converter is stopped by a timer which is used to prevent a decrement of efficiency in the proposed circuit.

V. DESIGN OF REACTORS

A. Design of reactors

In the proposed circuit, the ripple current of the reactors becomes a maximum value when the differential voltage between the fuel cell voltage and the output voltage are maximum. The value of the ripple current of the reactor do influence on the lifetime of the fuel cell.

Fig. 4 shows operation modes of the proposed circuit 1 and 2 in boost mode, respectively. In boost mode, the switch S_2 maintains at on state. The difference voltage is then controlled by PWM modulation of S_1 . The fuel cell current is sum of the current of the output reactor and the parallel converter current. The ripple current of the fuel cell Δi_{fc1} and Δi_{fc2} is obtained by (8) and (9), using the peak value of the parallel converter current Δi_{comp1} and Δi_{comp2} which are the discontinuous triangle waveform, and the ripple current of the output reactor are Δi_{Lout1} and Δi_{Lout2} while S_1 is on.

$$\Delta i_{fc1} = \Delta i_{comp1} + \Delta i_{Lout1} = \frac{V_{fc}}{L_{fc}} \frac{1}{f_{sw}} \left| \frac{V_{fc} - V_{out}}{V_{sb}} \right| \quad (8)$$

$$\begin{aligned} \Delta i_{fc2} &= \Delta i_{comp2} + \Delta i_{L_{out2}} \\ &= \left\{ \frac{V_{fc}}{L_{comp}} + \frac{1}{L_{out2}} (V_{fc} + V_{sb} - V_{out}) \right\} \frac{1}{f_{sw}} \frac{|V_{fc} - V_{out}|}{V_{sb}} \end{aligned} \quad (9)$$

From (8), the ripple current of the fuel cell in the proposed circuit 1 is inversely proportional to L_{fc} . From (9), the ripple current of the fuel cell in the proposed circuit 2 is inversely proportional to L_{comp} and L_{out2} . When both the ripple current of the fuel cell in the proposed circuit 1 and proposed circuit 2 are the same, L_{comp} which has same ripple current of the fuel cell in the proposed circuit 1 is obtained by (10).

$$L_{comp} = \frac{V_{fc}}{\frac{V_{fc}}{L_{fc}} - \frac{V_{fc} + V_{sb} - V_{out}}{L_{out2}}} \quad (10)$$

However, the denominator of (10) should be more than zero. Therefore, L_{out2} is obtained by (11).

$$L_{out2} > \frac{V_{fc} + V_{sb} - V_{out}}{V_{fc}} L_{fc} \quad (11)$$

Fig. 5 shows calculation results of the inductance values of L_{comp} and L_{out2} in the proposed circuit 2. Table I shows design specifications for the reactors. The calculation results confirmed that L_{comp} and L_{out2} should be more than $30\mu\text{H}$, $58.5\mu\text{H}$ while L_{fc} and L_{out1} is $30\mu\text{H}$, respectively. Note that the inductances of the reactors in the proposed circuit 2 are constrained by (10), (11). Therefore, the inductances of the reactors in the proposed circuit 2 are larger than the ones in the proposed circuit 1. Because L_{comp} contribute to suppression of the ripple current of the fuel cell only while S_1 is on. As a result, L_{out2} which always contribute in the suppression of the ripple current of the fuel cell should be larger. However, the current of L_{comp} does not include the direct current component. Therefore, the core which has a lower saturation magnetic flux density than the L_{out2} can be selected for use in L_{comp} . Therefore, in the proposed circuit 2, the inductance of L_{out2} should be smaller and the inductance of L_{comp} should be larger. However, the ripple current of L_{out2} increases if L_{out2} is small. As a result, the increasing of the copper loss which is caused by ripple component will be considered. However, major copper loss which is caused by the direct current component is reduced in Table I condition.

B. Maximum of the magnetic flux density of the core

In case of L_{fc} , the magnetic flux density of L_{fc} is obtained by (12).

$$\Delta B_{fc} = \frac{1}{N_1 S_1} \int V_{L_{fc}} dt \quad (12)$$

where N_1 is the number of wiring turns of L_{fc} , S_1 is the cross-section area of a core of L_{fc} and $V_{L_{fc}}$ is the reactor voltage. In addition, the reactor voltage is the square waveform in the proposed circuit. Therefore, (12) is also expressed by (13).

$$\Delta B_{fc} = \frac{V_{L_{fc}} t_{on}}{N_1 S_1} \quad (13)$$

where t_{on} is switch on time of S_1 . t_{on} is obtained from (14).

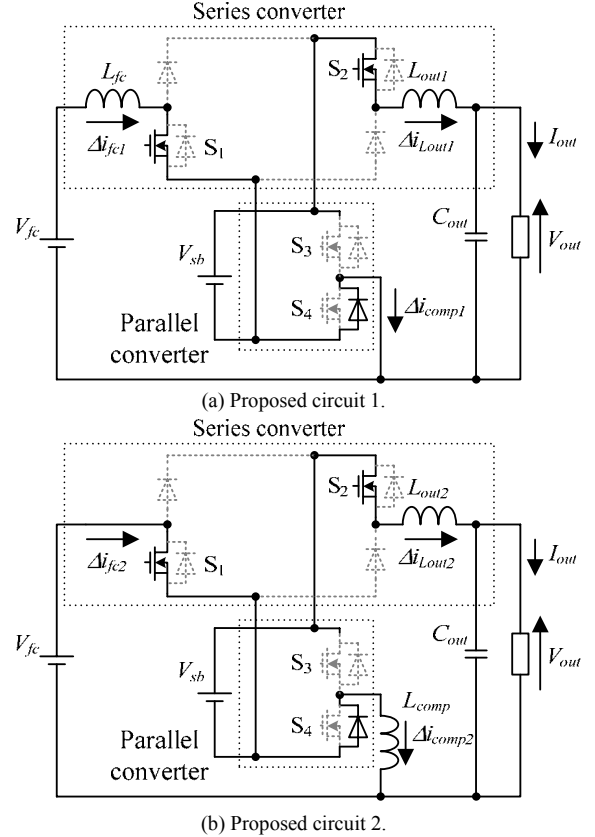


Fig. 4. Operation mode (Boost operation, S_1 is on).

TABLE I
SPECIFICATIONS FOR DESIGN OF REACTORS

Fuel cell voltage V_{fc}	4 to 10 (V)
Output power P_{out}	9.3 (W)
Output voltage V_{out}	7.2 (V)
Battery voltage V_{sb}	11 (V)
Switching frequency f_{sw}	100 (kHz)
Ripple current of the reactor Δi_{fc}	30% of output current (A)

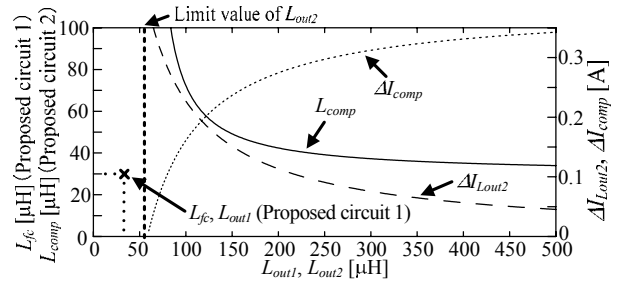


Fig. 5. Relation of inductances of the reactors and ripple current ($V_{fc}=4\text{V}$).

$$t_{on} = \frac{1}{f_{sw}} \frac{|V_{fc} - V_{out}|}{V_{sb}} \quad (14)$$

On the other hand, the direct current component of the magnetic flux density $B_{DC_{fc}}$ is proportional to reactor current. Therefore, it is obtained by (15) using (13).

$$B_{DC_fc} = \frac{\Delta B_{fc}}{\Delta i_{fc1}} I_{out} \quad (15)$$

where I_{out} is the output current which is the average current of the L_{out1} . Although the average current of L_{fc} is actually different from I_{out} , there is not much difference between the average current of L_{fc} and the output current I_{out} . Therefore, the maximum of the magnetic flux density B_{peak_fc} is expressed by (16) using (13), (15).

$$B_{peak_fc} = B_{DC} + \frac{\Delta B_{fc}}{2} = \frac{\Delta B_{fc}}{\Delta i_{fc}} I_{out} + \frac{\Delta B_{fc}}{2} = \frac{V_{Lfc} t_{on}}{N_1 S_1} \left(\frac{I_{out}}{\Delta i_{fc1}} + \frac{1}{2} \right) \quad (16)$$

In case of L_{comp} , the maximum flux density of L_{comp} is dominated by the peak of current of L_{comp} because it is a discontinuous triangle waveform. Therefore, the maximum magnetic flux density B_{peak_comp} is expressed by (17).

$$B_{peak_comp} = \frac{V_{Lcomp} t_{on}}{N_2 S_2} \quad (17)$$

where N_2 is the number of wiring turns of L_{comp} , S_2 is the cross-section area of a core of L_{comp} and V_{Lcomp} is the reactor voltage. In addition, V_{Lfc} and V_{Lcomp} are the same when on-resistance of the switch and forward voltage drop of the free wheeling diode (FWD) are considered to be negligible.

C. Comparison of cross-section area

Consideration on the theoretical volume of the reactors is conducted in this paper too. The reactor volume is depended on several factors which are the maximum magnetic flux density B_{peak_fc} , B_{peak_comp} , the cross-section area of the core S_1 , S_2 and the number of the wiring turns N_1 , N_2 , respectively. In order to compare the theoretical volume of the reactors between the proposed circuit 1 and 2, the cross-section area of the core is calculated in this section. For example, when both the maximum magnetic flux density B_{peak_fc} and B_{peak_comp} are the same, relations between the cross-section area of the core S_1 and S_2 is expressed by (18).

$$\frac{S_2}{S_1} = \frac{1}{\frac{N_2}{N_1} \left(\frac{I_{out}}{\Delta i_{fc1}} + \frac{1}{2} \right)} \quad (18)$$

In addition, S_1 is 24mm², N_1 is 13 turns.

Fig. 6 shows the calculation result of the cross-section area of the core. The calculation result confirmed that the cross-section of area of the core S_2 can be smaller than the core S_1 if the number of the wiring turns N_2 is larger than about a quarter of the number in the wiring turns N_1 .

VI. EXPERIMENTAL RESULTS

A. Series-parallel compensation operation

The proposed circuit was tested under the experimental conditions as shown in Table I. The response of the current regulator was designed as much higher than that of the LPF. It should be noted that the time constant was set to a shorter

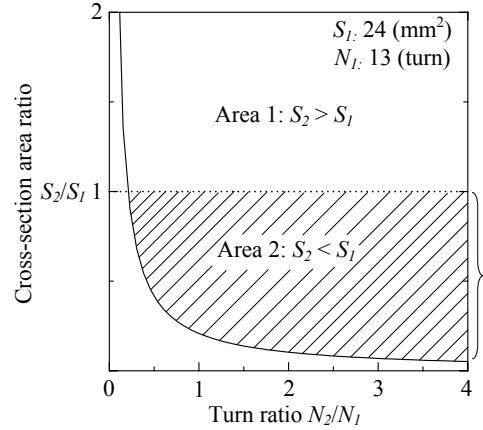


Fig. 6. Cross-section area of the core.

time in this experimental condition in order to confirm the effectiveness of the parallel converter. In order to reduce a negative influence on the lifetime of the fuel cell, the time constant should be set to a few seconds.

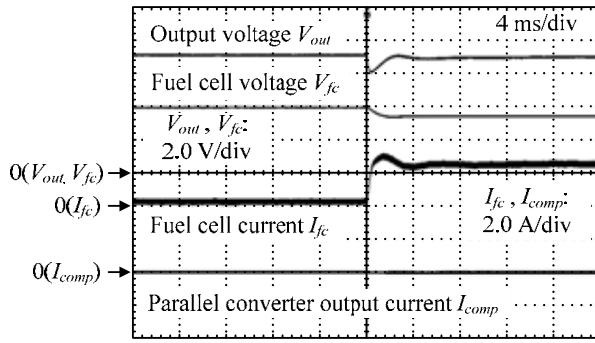
Fig. 7 shows waveforms of the fuel cell current and the output voltage with the parallel compensation when the load condition is changed in the proposed circuit 1. Fig. 4 confirmed that the variation of the fuel cell current is suppressed by the parallel compensation. The output voltage is kept constant by the PI regulator. The output voltage drops within 7% is known. It should be noted that the output voltage waveform has no low frequency component and the fluctuation is in a steady state load.

B. Efficiency of the proposed circuit

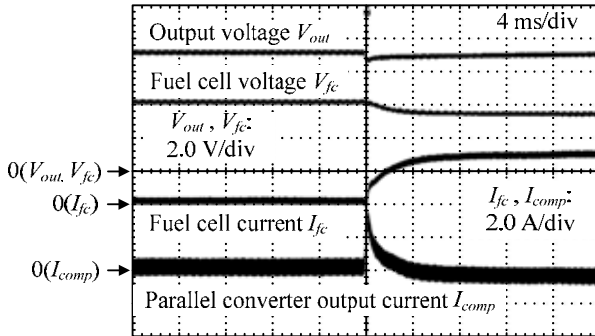
Fig. 8 shows the efficiency of the proposed circuits to confirm the effectiveness of the series compensation under the experimental conditions as shown in Table I. The experimental results confirmed that the proposed circuits could achieve 98.8% and 99.1% at the maximum efficiency point in the small differential voltage region, respectively. In the buck mode, the efficiency of the proposed circuit 2 is higher than that of the proposed circuit 1. In contrast, the efficiency of the proposed circuit 2 is lower than that of the proposed circuit 1 when the fuel cell voltage is in boost mode.

Fig. 9 shows equivalent circuits of the proposed circuit 1 and 2 in buck mode, respectively. In the proposed circuit 1, the current flows through the parallel converter. That is, the current flows through FWD of switch S_4 . On the other hand, the current does not flow through the FWD of S_4 in the proposed circuit 2. This reason is because the battery voltage is higher than the fuel cell voltage. As a result, FWD of S_4 in the proposed circuit 2 will not be an on state. Therefore, FWD loss in the parallel converter is not occurring. In addition, the loss of the reactor L_{comp} is not occurring either because the current does not flow through the parallel converter. As a result, the sums of the reactor loss in the proposed circuit 2 are reduced. Therefore, the efficiency of

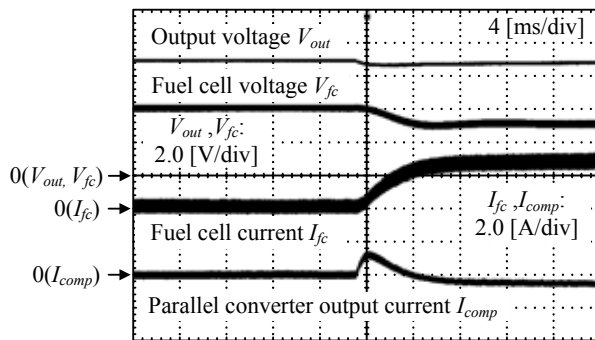
Parameter	Value
Fuel cell voltage V_{fc}	4 to 10 (V)
Output voltage V_{out}	7.2 (V)
Battery voltage V_{sb}	11 (V)
Switching frequency f_{sw}	100 (kHz)
Input reactor L_{fc}	30 (μ H)
Parallel converter reactor L_{comp}	30 (μ H)
Output reactor L_{out1}, L_{out2}	30 (μ H)
Output capacitor C_{out}	800 (μ F)
AVR response	0.1 (kHz)
ACR response	1 (kHz)
LPF time constant	2.2 (ms)
Load change	2 to 20 (W)



(a) Series compensation only (proposed circuit 1).



(b) Series-parallel compensation (proposed circuit 1).



(c) Series-parallel compensation (proposed circuit 2)

Fig. 7. Voltage waveforms and current waveforms for increasing output power.

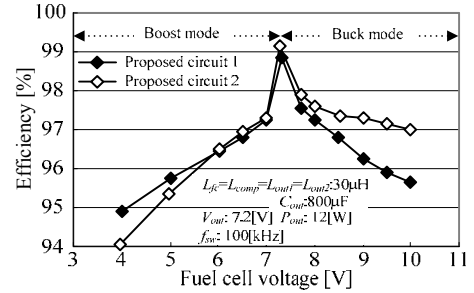
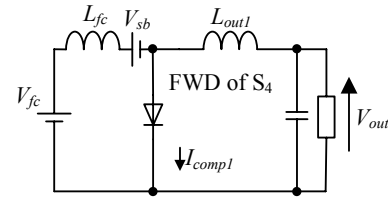
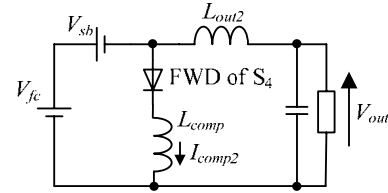


Fig. 8. Efficiency of the proposed circuit.



(a) Proposed circuit 1.



(b) Proposed circuit 2.

Fig. 9. Equivalent circuit of the proposed circuit in buck mode.

circuit 1 in the buck mode.

C. Loss analysis

In order to evaluate the power loss of the proposed circuit, the loss measurement and analysis for each part was implemented under the experimental conditions as shown in Table I. Fig. 10 shows the result of the loss analysis. The features of the proposed circuits are the copper loss and the iron loss of the reactors could achieve minimum loss in the small differential voltage region ($V_{fc}=7.3V$), the proposed circuit is able to obtain high efficiency. From the loss analysis, the efficiency of the proposed circuit 2 is higher than the proposed circuit 1 in buck mode, because the loss of the reactor has been decreased. On the other hand, in boost mode, although the copper loss of the reactor is decreased in the proposed circuit 2, the efficiency of the proposed circuit 2 is lower than the proposed circuit 1. The reason for low efficiency in the proposed circuit 2 when the fuel cell voltage is 4V in the boost mode is that the power loss is increased because of the increasing of iron loss in the reactor. In conclusion, the proposed circuit 1 is superior for the boost mode. Then the input voltage has a longer operation time of lower voltage to the output voltage. On the opposite, the circuit 2 is suitable for the buck mode.

the proposed circuit 2 is higher than that of the proposed

D. Ripple current of the fuel cell

Fig. 11 shows the waveforms of the fuel cell current in the proposed circuit 1 and 2, respectively. The experimental results confirmed that the fuel cell current contains a ripple with 100 kHz switching frequency.

Fig. 12 shows the experimental results of the ripple fuel cell current of the proposed circuit 1 and the proposed circuit 2, respectively. The experimental results confirmed that the designed reactor could suppress the ripple current of the fuel cell within the set value. Furthermore, the theoretical value agrees with the experimental results.

VII. CONCLUSION

A series-parallel compensation type DC-DC converter has proposed to achieve high efficiency, downsizing and longer lifetime in an application of a fuel cell-battery hybrid system. When the output power is almost constant, the series converter provides only the differential voltage between the fuel cell voltage and the output voltage, while the parallel converter suppresses the variation of the fuel cell current.

The experimental results confirmed that the proposed circuit could achieve a maximum efficiency of 98.8% and 99.1% in the small differential voltage region. In addition, from the loss analysis, it is confirmed that the optimizing of the reactor is needed in order to improve the efficiency of the proposed circuit. The proposed circuit 2 is superior in term of efficiency for the buck operation mode and direct operation mode. In addition, the design of the reactors is discussed and the suppression of the ripple in the fuel cell current has been confirmed with the theoretical calculation and experimental results.

REFERENCES

- [1] Yilei Gu, Zhengyu Lu, and Zhaoming Qian, "Three Level LLC Series Resonant DC/DC Converter," Proc. of IEEE-APEC04, pp. 1647- 1652
- [2] Eui-Sung Kim, Dong-Yun Lee, and Dong-Seok Hyun, "A Novel Partial Series Resonant DC/DC Converter with Zero-Voltage/Zero-Current Switching," Proc. of IEEE-APEC00, pp. 93- 98
- [3] Jiann-Fuh Chen, Wei-Shih Liu, Ray-Lee Lin, Tsomng-Juu Liang, and Ching-Hsiung Liu, "High-Efficiency Cascode Forward Converter of Low Power PEMFC System," Proc. of IEEE-IPEMC06
- [4] Changrong Liu, Amy Johnson, and Jih-Sheng Lai, "A Novel Three-Phase High-Power Soft-Switched DC/DC Converter for Low-Voltage Fuel Cell Applications," *IEEE Trans. Industry Applications*, pp. 1691-1697, 2005
- [5] Xin Kong, Ashwin M. Khambadkone, "Analysis and Implementation of a High Efficiency, Interleaved Current-Fed Full Bridge Converter for Fuel Cell System," *IEEE Trans. Power Electronics*, pp. 543- 550, 2007
- [6] H. Tao, A. Kotsopoulos, J. L. Duarte, and M. A. Hendrix, "A Soft-Switched Three Port Bidirectional Converter for Fuel Cell and Supercapacitor Applications," Proc. of IEEE-PESC05, pp. 2487- 2493
- [7] Naehyuck Chang, "Fuel Cell and Battery Hybrid System for Portable Electronics Applications," 10th Annual International Conference SMALL FUEL CELLS 2008 – Portable & Micro Fuel Cells for Commercial & Military Applications, 2008
- [8] Zhenhua Jiang, Lijun Gao, and Roger A. Dougal, "Flexible Multiobjective Control of Power Converter in Active Hybrid Fuel Cell/Battery Power Sources," Proc. of IEEE-PESC04, pp. 3804- 3811

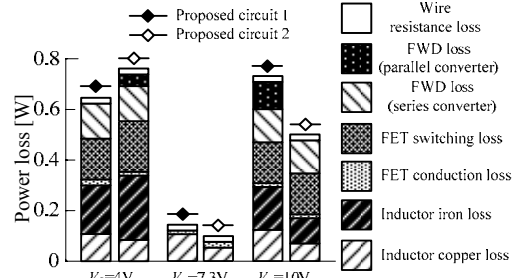
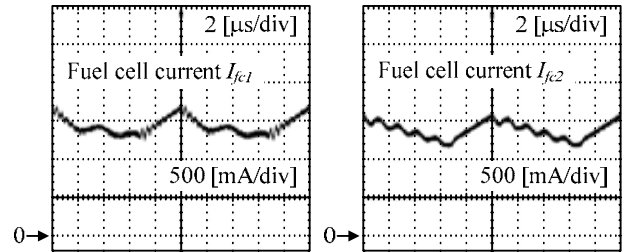
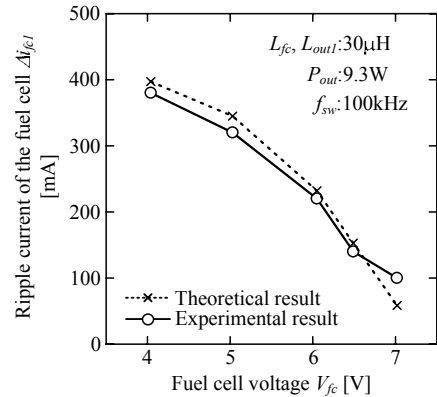


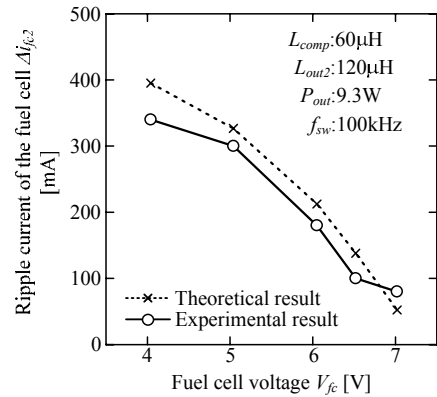
Fig. 10. Loss analysis of the experimental result.



(a) Proposed circuit 1. (b) Proposed circuit 2.
Fig. 11. Current waveforms of the fuel cell ($V_{fc}=4V$).



(a) Proposed circuit 1.



(a) Proposed circuit 2.

Fig. 12. Comparison of the ripple current of the fuel cell.

- [9] Koji Orikawa, Jun-ichi Itoh, "High efficiency DC-DC converter using a series-parallel compensation method for a fuel cell," The 13th European Conference on Power Electronics and Applications, pp. 1-9